SUPPORTING INFORMATION

The *Streptomyces*-produced antibiotic fosfomycin is a promiscuous substrate of archaeal isopentenyl phosphate kinase

Mark F. Mabanglo[1], Adrian W. R. Serohijos[2] and C. Dale Poulter[1*]

[1]Department of Chemistry, University of Utah, 315 South 1400 East Salt Lake City, Utah 84112 USA [2]Department of Chemistry and Chemical Biology, Harvard University, 12 Oxford Street, Cambridge, Massachusetts 02138 USA.

TABLE OF CONTENTS

EXPERIMENTAL PROCEDURES

Materials. γ-[^{32}P-ATP] was purchased from American Radiolabeled Chemicals. Disodium salts of fosfomycin (>99%), phosphoenolpyruvate (PEP) and nicotinamide adenine dinucleotide (NADH) were purchased from Sigma-Aldrich. Bovine serum albumin was purchased from Invitrogen. Lactate dehydrogenase (rabbit muscle) and pyruvate kinase (rabbit muscle) were purchased from Roche. The concentrations of all reagents containing phosphates were determined by phosphate analysis, and the precise concentration of stock IPK enzyme was measured using the BCA Protein Assay Kit from Pierce. Synthesis of IP and the cloning, expression and purification of THA IPK were performed using the same procedures as in *(1)*. The expressed THA IPK protein, including mutants, all contained an N-terminal 6×Histidine tag and a thrombin recognition sequence and were purified to homogeneity (99%).

Competitive inhibition of IP kinase activity by fosfomycin. Different concentrations of IP and fosfomycin were added to the assay buffer (100 mM HEPES pH 7.5 containing 10 mM $MgCl_2$, 10 mM β-mercaptoethanol and 1 mg/mL BSA). The reaction was initiated by mixing a solution of IPK in the same buffer with the first solution followed by incubation at 37 ^{o}C for 600 s. Initial rates were measured as in the procedure for the fluorescence assay, and the inhibition constant K_i was determined by fitting the initial rate matrices to the equation for competitive inhibition:

$$\nu = V_{max}\,[S] / [S] + K_m(1 + [I]/K_i) \qquad (1)$$

where S is the substrate IP and I is the competitive inhibitor fosfomycin.

Site-directed mutagenesis of THA IPK. To create the K14A and K204A mutants, the forward primers 5'-GGCGGAAGCGTGATCACCGATGCATCCGCTTACCG'-3' and 5'-GTTACCGGCGGTATAGGGGCGAAGTTCGAATCCATGGT-3' were designed. PCR reactions were carried out following the protocol in the Quikchange Site-Directed Mutagenesis Kit manual (Stratagene).

Figure S1. Sequence alignment of four members of the amino acid kinase family of enzymes, *T. acidophilum* IPK (3LKK), *M. thermautotrophicus* IPK (3LL9), *S. wedmorensis* FomA (3D41) and *E. coli* NAGK (1GS5). Missing residues (189-201) in IPK (green box) were modeled using the aligning region in NAGK (red box). Sequence alignment was generated using ClustalW2 *(2)* and ESPript *(3).*

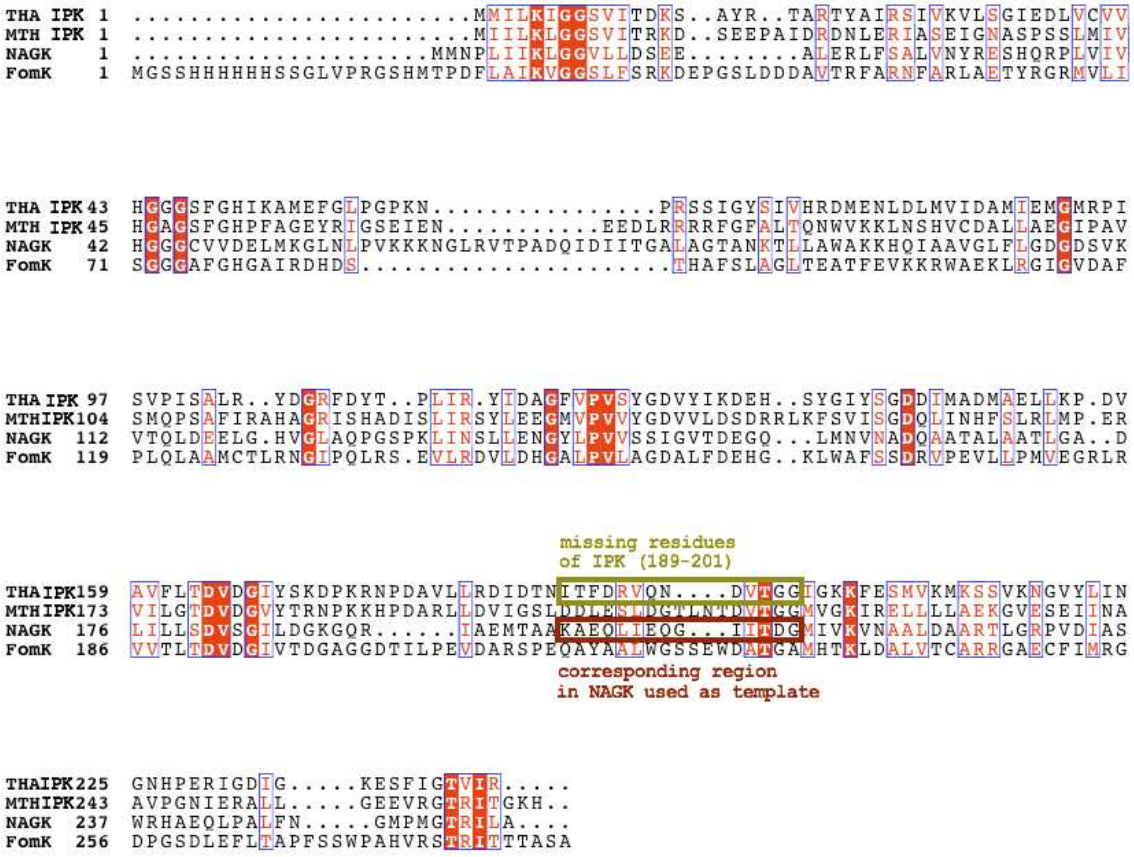

Figure S2. Superposition of IPK (3LKK, green) and NAGK (1GS5, red) structures shows high homology. The αF helix of NAGK and the connecting loop (residues 200-213) flow almost seamlessly into the αG helix of IPK, suggesting that it is a good template to model the missing residues of IPK (189-201). Image was generated using PyMOL *(4)*.

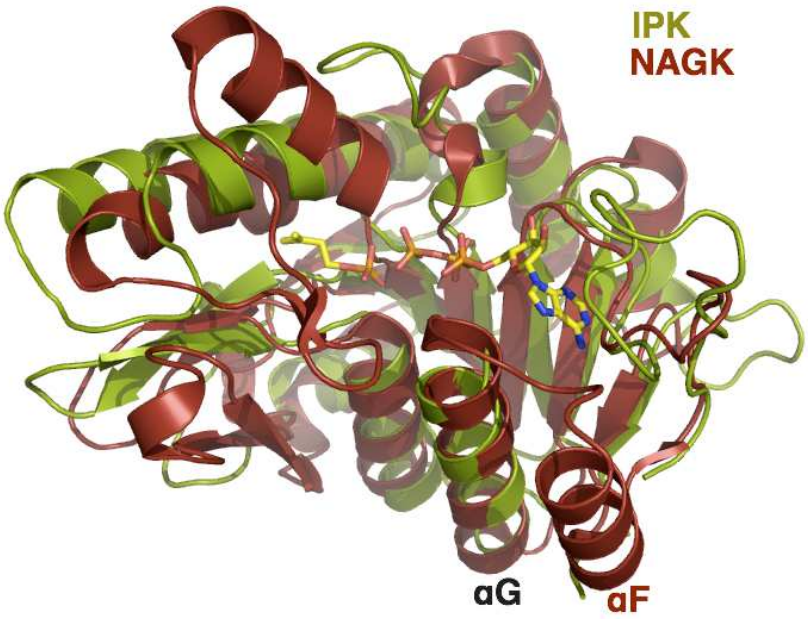

Figure S3. MS/MS fragmentation of fosfomycin standard. Species corresponding to $[C_3H_5O]^+$ (56.9) and $[C_3H_6O_3P]^+$ (120.8), also found in the fragmentation of fosfomycin phosphate produced by THA IPK and *S. wedmorensis* FomA, are indicated.

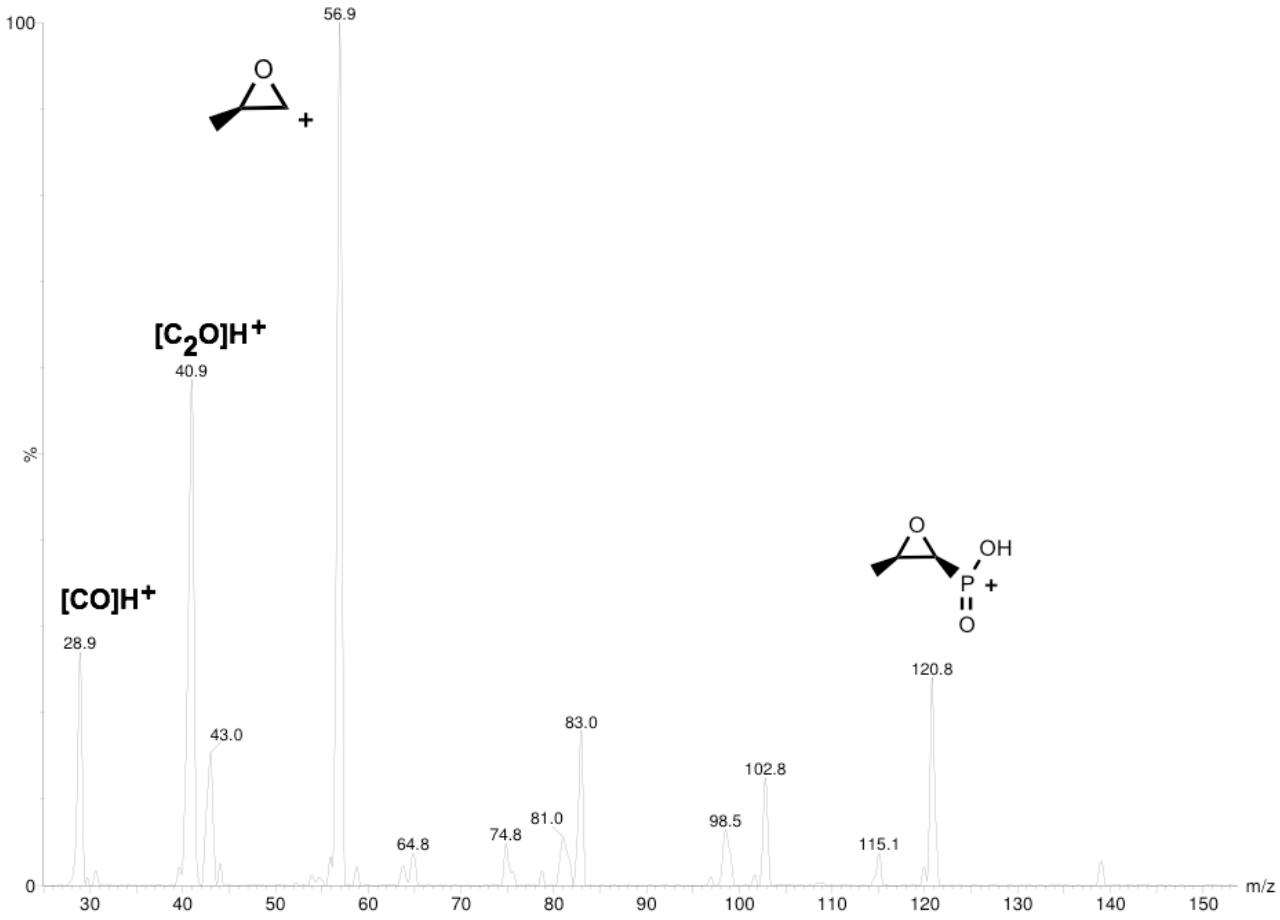

Figure S4. Fosfomycin is a promiscuous substrate of IPK. (a) Michaelis Menten curve showing saturation of IPK at high mM concentrations of fosfomycin. A high K_m (15.1 mM) indicates weak binding of fosfomycin to the IP binding site. (b) Lineweaver-Burk transformation of (a), indicating a sequential binding mechanism and formation a ternary complex of IPK•fosfomycin•ATP. (○) 2 μM ATP, (●) 4 μM ATP, (□) 6 μM ATP, (■) 8 μM ATP.

a

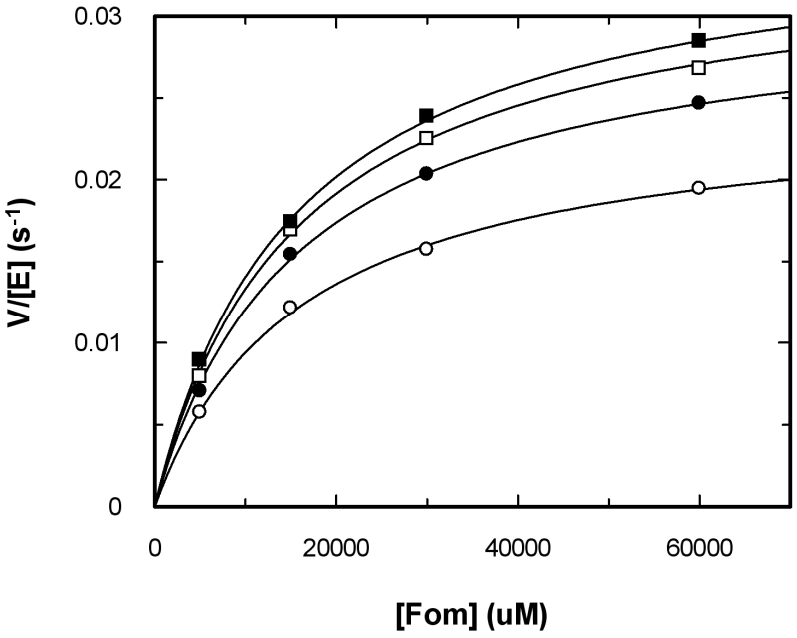

b

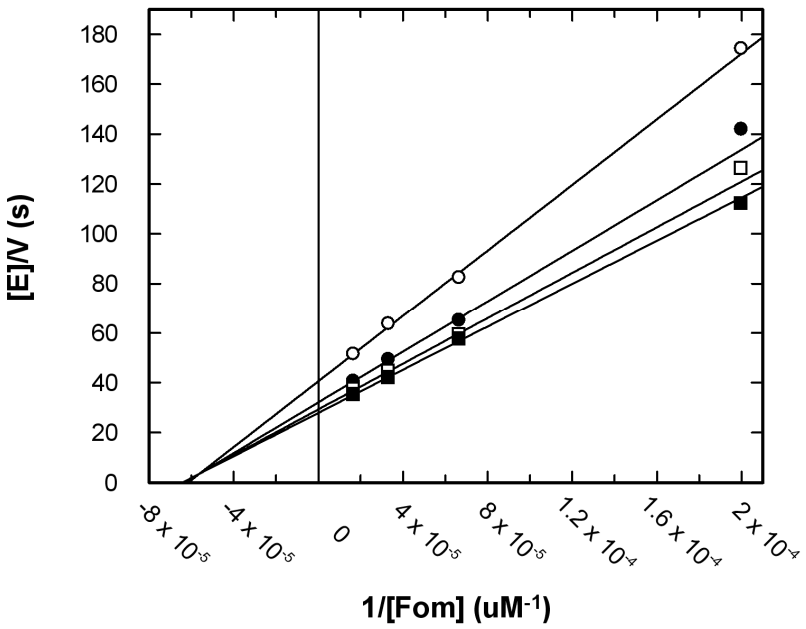

Figure S5. Fosfomycin is a competitive inhibitor of IPK. (a) Michaelis Menten curve showing an increase in K_m^{IP} with increasing fosfomycin concentration. (b) Lineweaver-Burk transformation of (a) showing a family of lines intersecting at the y-axis, indicating a constant V_{max}. (○) 0 mM fosfomycin, (●) 1 mM fosfomycin, (□) 2 mM fosfomycin, (■) 3 mM fosfomycin, (△) 4 mM fosfomycin.

a

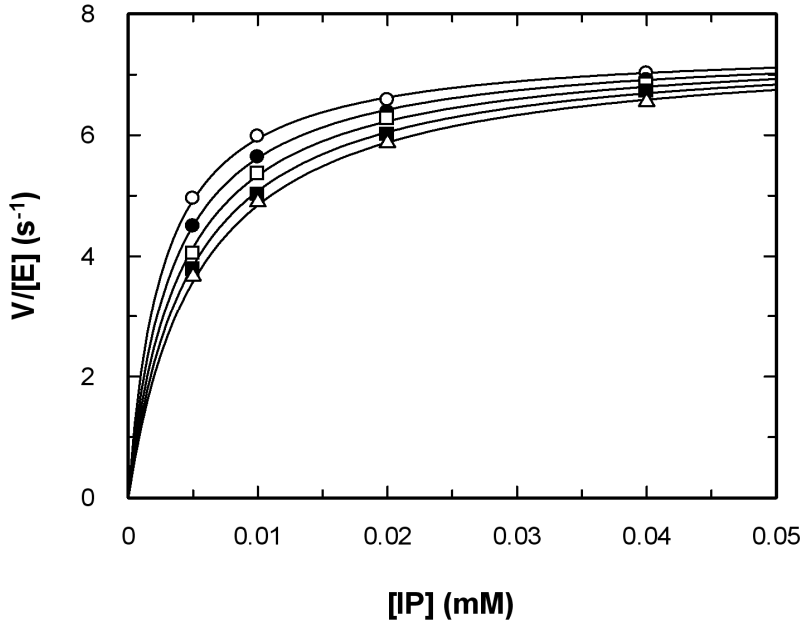

b

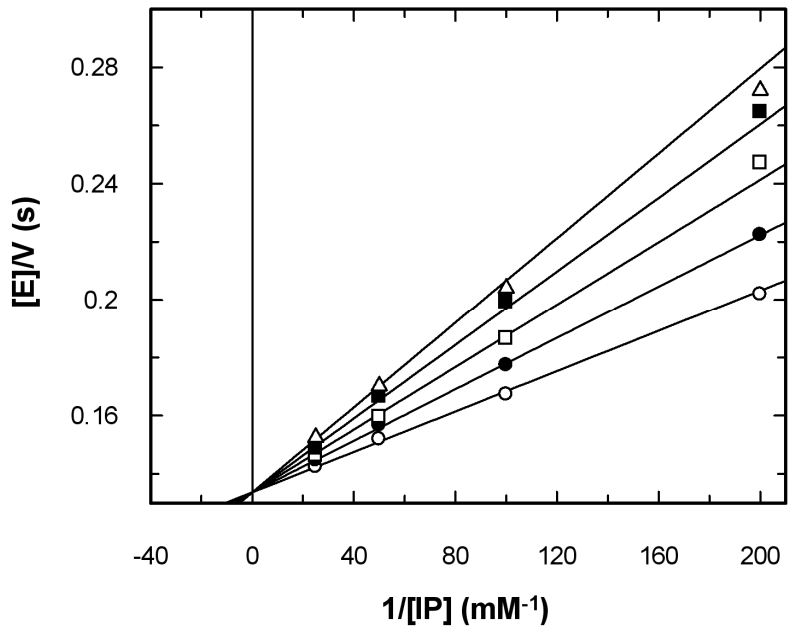

Figure S6. The modeled IPK•IP•MgATP complex is stable with only one binding pose for IP in the active site. (a) RMSD time-series showing that the modeled IPK•IP•MgATP complex is stable. (b) Ligand (IP and ATP) RMSD showing a single-state binding conformation for IP and ATP.

a

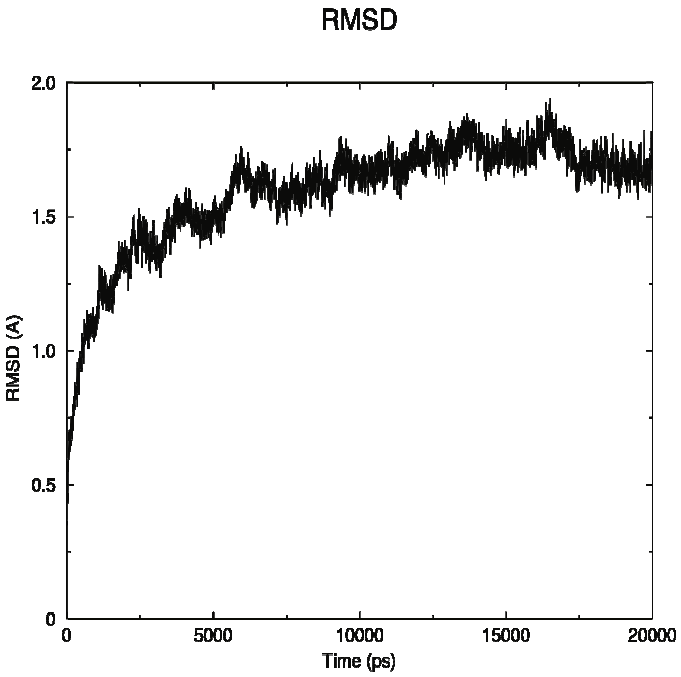

b

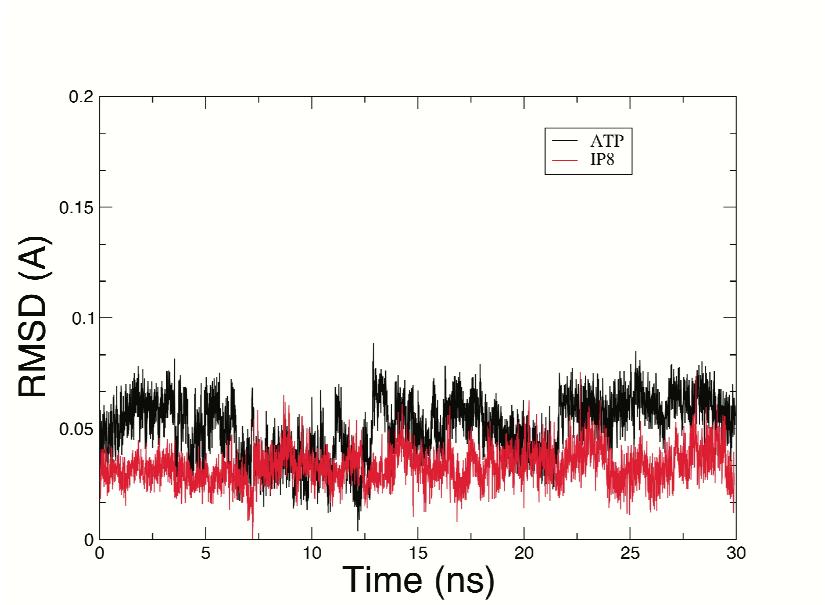

Figure S7. Kinetic studies on the K204A mutant with fosfomycin and IP. (a) Kinetic measurements using fosfomycin as substrate showed that the mutant can catalyze the promiscuous reaction to the same extent as native THA IPK. (○) 2 μM ATP, (●) 4 μM ATP, (□) 6 μM ATP, (■) 8 μM ATP. (b) The K204A mutant can catalyze the native reaction (using IP as substrate) to the same extent as native THA IPK. (○) 10 μM ATP, (●) 20 μM ATP, (□) 40 μM ATP, (■) 80 μM ATP.

a

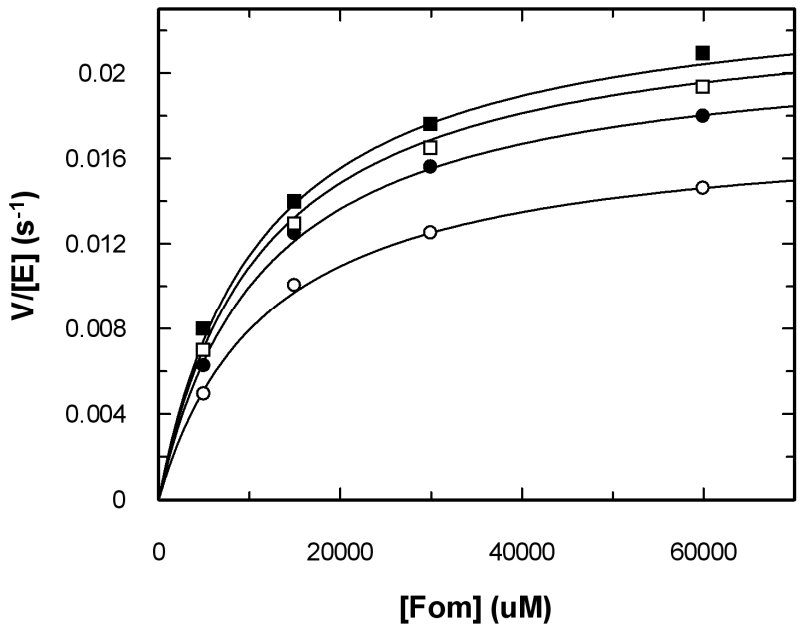

b

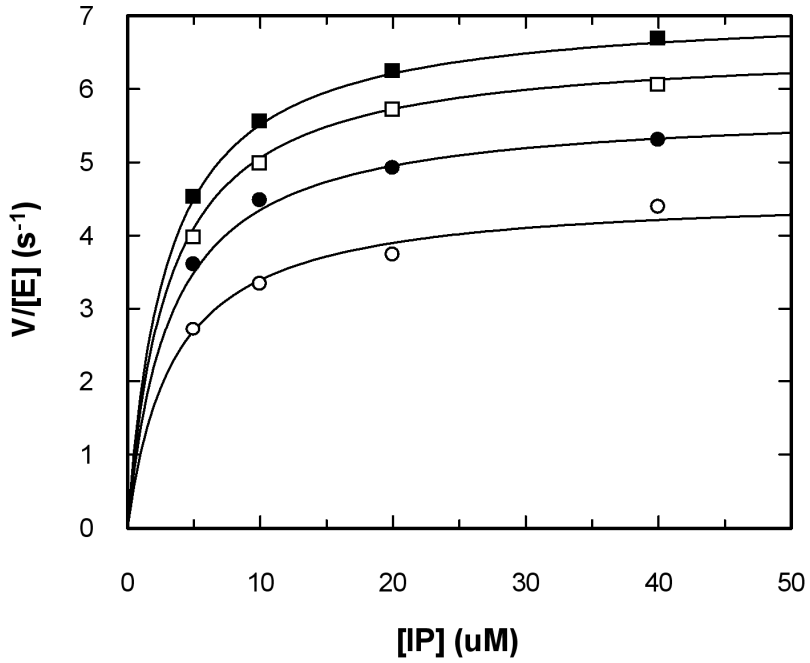

Figure S8. Michaelis Menten curves and kinetic constants of the K14A THA IPK mutant. (○) 10 μM ATP, (●) 20 μM ATP, (□) 30 μM ATP, (■) 40 μM ATP.

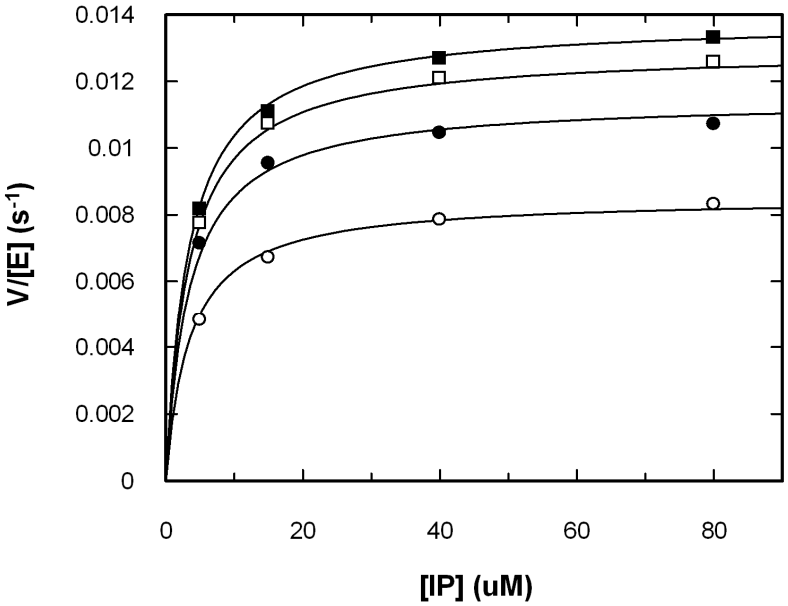

Table S1. Kinetic constants for the K14A THA IPK mutant using IP as substrate.

k_{cat} (s^{-1})	$(2 \pm 0.04) \times 10^{-2}$
K_m^{IP} (μM)	3.2 ± 0.5
k_{cat}/K_m ($M^{-1}s^{-1}$)	5.453×10^{3}
K_m^{ATP} (μM)	10.5 ± 0.8
K_d^{IP} (μM)	3.8 ± 1.1

REFERENCES

1. Chen, M., and Poulter, C.D. *Biochemistry* **2010**, *49*, 207-217.

2. Larkin, M. A., Blackshields, G., Brown, N. P., Chenna, R., , McGettigan, P. A., McWilliam, H., Valentin, F., Wallace, I. M., Wilm, A., Lopez, R., Thompson, J. D., Gibson, T. J., and Higgins, D. G. Clustal W and Clustal X version 2.0. *Bioinformatics* **2007**, *23 (21)*, 2947-2948.

3. Gouet, P., Courcelle, E., Stuart, D.I., and Metoz, F. *Bioinformatics* **1999**, *15(4)*, 305-308.

4. DeLano, W. L. *The PyMOL Molecular Graphics System*, DeLano Scientific, Palo Alto, CA, USA, **2002**.

5. MacKerell, A. D., Jr.; Bashford, D.; Bellott, M.; Dunbrack, R. L., Jr.; Evanseck, J.; Field, M. J.; Fischer, S.; Gao, J.; Guo, H.; Ha, S.; Joseph, D.; Kuchnir, L.; Kuczera, K.; Lau, F. T. K.; Mattos, C.; Michnick, S.; Ngo, T.; Nguyen, D. T.; Prodhom, B.; Reiher, W. E., III.; Roux, B.; Schlenkrich, M.; Smith, J.; Stote, R.; Straub, J.; Watanabe, M.; Wiorkiewicz-Kuczera, J. Yin, D., and Karplus, M. *J. Phys. Chem. B* **1998**, *102*, 3586−3616.